they are found to lie in the upper critical region predicted by the theoretical curve. Second virial coefficients $A_2$, for the 2.2 acetate–acetone system, were also measured at a fixed temperature of 296°K for a range of molecular weights. These varied in the manner shown in Figure 6, which indicates that the solubility limit is above 80,000 and that $A_2 = 0$ for $\bar{M}_n \sim 10{,}000$. This latter value is also plotted in Figure 4 and again lies on the theoretical curve.

Of course this agreement may be completely fortuitous. On the other hand as over 25% of the side groups in the chain are hydroxyls the 2.2 acetate can be regarded effectively as a copolymer. As such, one would expect a complex interaction to exist between the polymer and solvent with both hydroxyl and acetyl groups behaving in different ways. Moore[13] showed that the secondary acetate was heavily solvated by acetone and that seven solvent molecules were associated with each partially substituted glucose residue. This suggests that there is a strong interaction between solvent and polymer which may involve hydrogen bonding between the hydroxyl groups and acetone in addition to the interaction between the solvent and the acetyl groups. For random copolymers it has been suggested that the solubility behavior can be anticipated by averaging the separate homopolymer solubility parameters according to the copolymer composition, and so a copolymer consisting of polar and nonpolar residues will dissolve in solvents of intermediate polarity such as acetone.

Consequently the secondary acetate behaves partly like the primary acetate, exhibiting LCS behavior below which there is a region of miscibility which would normally finish as predicted by the theoretical curve and the decreasing $A_2$. Before the polymer can precipitate, as the temperature decreases further, the interaction of the hydroxyl groups with acetone enhances the solubility and prevents phase separation at the expected temperatures. This secondary solvation depresses the UCST for each sample until phase separation eventually occurs at temperatures much lower than expected. While it is unlikely that hydrogen bonding is the sole cause of the solvation, as the suggested phase separation temperatures are as high as 80° for certain samples, it probably becomes increasingly important at lower temperatures.

The degree of substitution in the cellulose molecule has a significant effect on the precipitation temperatures. In the lower critical region a decrease in DS results in a decrease in LCST; a similar trend is observed in the upper critical region.

The application of the Prigogine theory to phase separation in these systems is thus moderately successful, particularly for the primary acetate, but the complications introduced by the copolymeric character of the secondary acetate do not allow a critical assessment of this system to be made at present, especially as the polymer is semipolar and the theoretical approach is derived primarily for nonpolar systems.

(13) W. R. Moore, *J. Polym. Sci., Part C*, **No. 16**, 571 (1967).

# Kinetics of Autoxidation of Atactic Polypropylene in the Presence of Cobalt Salts by Infrared Spectroscopy

**S. S. Stivala,[1a,b] B. R. Jadrnicek,[1b] and Leo Reich[1c]**

*Department of Chemistry and Chemical Engineering, Stevens Institute of Technology, Hoboken, New Jersey 07030, and Polymer Research Branch, Picatinny Arsenal, Dover, New Jersey 07801.* *Received July 24, 1970*

ABSTRACT: A general scheme previously reported for the uncatalyzed autoxidation of polyolefins was modified to account for the metal-catalyzed [cobalt(III) acetylacetonate] autoxidation of atactic polypropylene (APP). This modified scheme yielded various kinetic expressions relating a net maximum rate of carbonyl formation ($\rho_{m,net}$) as a function of catalyst and oxygen concentrations. These expressions could satisfactorily account for the experimental data obtained. The reaction temperature ranged from 100 to 130°, the metal concentration from (0.3 to 82.0) $\times 10^{-7}$ mol/7.5 mg of APP, and the oxygen concentration [$O_2$] from 5 to 100 vol %. As anticipated, at relatively low catalyst concentrations [Cat.], $\rho_{m,net}$ was approximately first order in respect to [Cat.] and about zero order in [Cat.] at relatively high values of [Cat.]. Further, a satisfactory relationship between $\rho_{m,net}$ and [$O_2$] could be obtained.

Mathematical expressions derived from a general kinetic scheme have been satisfactorily applied to the uncatalyzed autoxidation of polyolefins such as polypropylene[2,3] and polybutene[2a,4,5] in the bulk phase. This scheme was recently modified by Bawn and Chaudhri[6] to account for the kinetics of manganese salts catalyzed autoxidation of atactic polypropylene

(1) (a) To whom correspondence should be addressed; (b) Stevens Institute of Technology; (c) Picatinny Arsenal.

(2) (a) L. Reich and S. S. Stivala, "Autoxidation of Hydrocarbons of Polyolefins," Marcel Dekker, New York, N. Y., 1969; (b) S. S. Stivala, L. Reich, and P. G. Kelleher, *Makromol. Chem.*, **59**, 28 (1963).

(3) B. R. Jadrnicek, S. S. Stivala, and L. Reich, *J. Appl. Polym. Sci.*, in press.

(4) S. S. Stivala, E. B. Kaplan, and L. Reich, *ibid.*, **9**, 3557 (1965).

(5) S. S. Stivala, G. Yo, and L. Reich, *ibid.*, **13**, 1289 (1969).

(6) C. E. H. Bawn and S. A. Chaudhri, *Polymer*, **9**, 81 (1968).

(APP) in solution. Other workers[2a,7-10] have also investigated the metal-catalyzed autoxidation of polyolefins, but in a relatively qualitative manner. The purpose of this paper is to extend the modified general scheme, in a quantitative manner, to the cobalt(III) acetylacetonate catalyzed autoxidation of APP in the bulk phase.

## Experimental Section

**A. Starting Materials. 1. Atactic Polypropylene (APP).** An uninhibited sample of APP, obtained from Avisun Corp., was refluxed with diethyl ether for 2 hr and insoluble residue (presumably an isotactic fraction) was removed by filtration through glass wool. The resulting filtrate was slowly added to methanol to precipitate the APP. The precipitate was repeatedly washed with methanol and dried at room temperature under vacuum. The dried APP was redissolved in diethyl ether, reprecipitated, and rewashed with methanol. This procedure was repeated once more. The dried APP was finally purified by passing its ether solution through a column of aluminum oxide. The APP was precipitated from the resulting eluent and dried under vacuum at 40° for 2 hr.

The yield, based on the original weight of APP, was about 60 wt %. An infrared spectrum of the dried APP was similar to that reported by Luongo.[11] From this spectrum it was ascertained, using the bands at 974 and 995 $cm^{-1}$, [11] that the sample was close to 100% atactic. Upon ignition, the APP sample gave an ash content of 0.008%, and by the use of a membrane osmometer a number average molecular weight of 30,000 was obtained.

**2. Metal Salt Catalyst.** Cobalt(III) and cobalt(II) acetylacetonates (2,4-pentanediones) were obtained from J. T. Baker Chemical Co. (highest purity grade) and were used without further purification, mp [Co(III) salt] 210–213°.

**B. Apparatus.** Infrared spectra were obtained from a Perkin-Elmer recording spectrophotometer, Model 21. Attached to this instrument was an oxidation cell which was essentially similar to that described previously.[2a] Briefly, the cell consists of a brass cylindrical body into which are introduced a standard salt plate, an aluminum spacer, a salt plate holder, a second salt plate containing the film specimen, and a threaded lock ring, respectively. The body of the cell is equipped with a temperature-controlling thermistor, reaction-temperature-indicating thermistor, and numerous turns of heating wire. A 0.25-in. metallic orifice perpendicular to the main body of the cell is used to admit gas, *e.g.*, $O_2$ and $O_2$–$N_2$, and a second smaller opening at the opposite end permits the escape of the gas. The temperature controller, Thermonitor Model ST (E. H. Sargent & Co.), had a temperature range up to 150° with a nominal temperature variation of ±0.05°. The cell chamber temperature was measured with an iron–constantan thermocouple connected to a Millivolt potentiometer (Leeds & Northrup). The Thermonitor temperature reading was calibrated against the potentiometer.

For the quantitative estimation of carbonyl content in the oxidized APP as ketones and aldehydes in the form of hydrazones, a Beckman DU spectrophotometer, Model 2400, was used.[3]

**C. Procedure.** Purified APP was dissolved in carbon tetrachloride and a portion of this solution was poured onto an optical sodium chloride disk attached to which was a Teflon gasket serving as a mold. Immediately following, a solution of either cobalt(III) or cobalt(II) acetylacetonate in carbon tetrachloride was added to the mold. Films about 2.5 mils thick were obtained by the slow evaporation of the solvent at room temperature and by drying under vacuum for *ca.* 30 min. The films on the sodium chloride disks were assembled in the oxidation cell which was then attached to the infrared spectrophotometer. Known amounts of purified oxygen and nitrogen mixtures (purified by means of sodium hydroxide and anhydrous calcium chloride) were passed into the oxidation cell at a constant rate of 30 ml/min after the desired reaction temperature had been reached. (Prior to reaching this temperature, the APP sample was heated under a blanket of nitrogen.) The ratios (by volume) of oxygen to nitrogen mixtures used were 5:95, 10:90, 25:75, 50:50, 75:25, and 100:0. The catalyst content in the film was varied from (0.3 to 82.0) $\times 10^{-7}$ mol/7.5 mg of APP. Reaction temperatures ranged from 100 to 130°. Infrared spectra of the carbonyl region were recorded as a function of reaction time, at a constant catalyst concentration, for different temperatures and $O_2$:$N_2$ ratios; *cf.* Figures 1 and 2. Further, at a constant temperature of 110° and at $O_2$:$N_2$ ratios of 100:0 and 50:50, carbonyl concentration was determined as a function of reaction time for various metal catalyst concentrations; *cf.* Figure 3. Apparent weight losses of APP films during oxidation were found to be low (<1%).

The character of the infrared carbonyl absorption band (5.4–6.1 μ) was generally the same as that obtained for the uncatalyzed oxidation of APP.[3] The amount of carbonyl (from aldehydes, acids, etc.) formed as a function of time was measured in terms of the total absorbance area (arbitrary units of $cm^2$) of the carbonyl band as described previously.[3] Further, based upon work reported for the uncatalyzed oxidation of APP, the following should be valid for the metal salt catalyzed oxidation of APP: (a) the Lambert–Beer law holds; (b) diffusion control does not apply to the 2.5-mil thick APP film under the various experimental conditions employed; (c) no oxidation products containing ester moieties could be detected. This implies that alkoxy radicals, RO· (*cf.* step 7), are not important in the formation of alcohols since these alcohols could presumably react with acid products to afford esters.

The amounts of various carbonyl-containing species were estimated by the same technique employed for the uncatalyzed oxidation of APP. In this manner, the following results were obtained under various experimental conditions: aldehydes and ketones ≈ 15 wt %, acids ≈ 85 wt % (by difference). (These values are similar to those found in the uncatalyzed APP oxidation;[3] further, it is tacitly assumed that the formation of carbonyl (as aldehyde and ketone) is the rate-controlling step *vis-à-vis* the rapid secondary oxidation of carbonyl groups to acids.) Thus, absorbance areas (5.4–6.1 μ) are directly proportional to total carbonyl concentration. Under the experimental conditions employed, the maximum conversion (up to the maximum rate of carbonyl formation) was *ca.* 2 wt % as carbonyl.

The weight per cent of hydroperoxide (as peroxidic oxygen) was estimated as follows.[12] Briefly, an APP sample was added to isopropyl alcohol, followed by 1 ml of saturated KI and 1 ml of glacial acetic acid. The mixture was heated almost to boiling, kept at incipient boiling for *ca.* 5 min, and then titrated without cooling with standard sodium thiosulfate to the disappearance of the yellow color.

## Theory

Equations 5–9 represent a general scheme[2b,3] that was modified to account for the experimental results ob-

(7) S. A. Chaudhri, *Polymer*, **9**, 604 (1968).
(8) Y. Kamiya, *J. Polym. Sci., Part B*, **4**, 999 (1966).
(9) Z. Osawa, T. Shibamiya, and K. Matsuzaki, *Kogyo Kagaku Zasshi*, **71**, 552 (1968).
(10) L. L. Yasina, V. B. Miller, and Y. A. Shlyapnikov, *Izv. Akad. Nauk SSSR*, **11**, 2635 (1968).
(11) J. P. Luongo, *J. Appl. Polym. Sci.*, **3**, 302 (1960).
(12) B. R. Jadrnicek, Ph.D. Thesis, Institute of Macromolecular Chemistry, Prague, 1967.

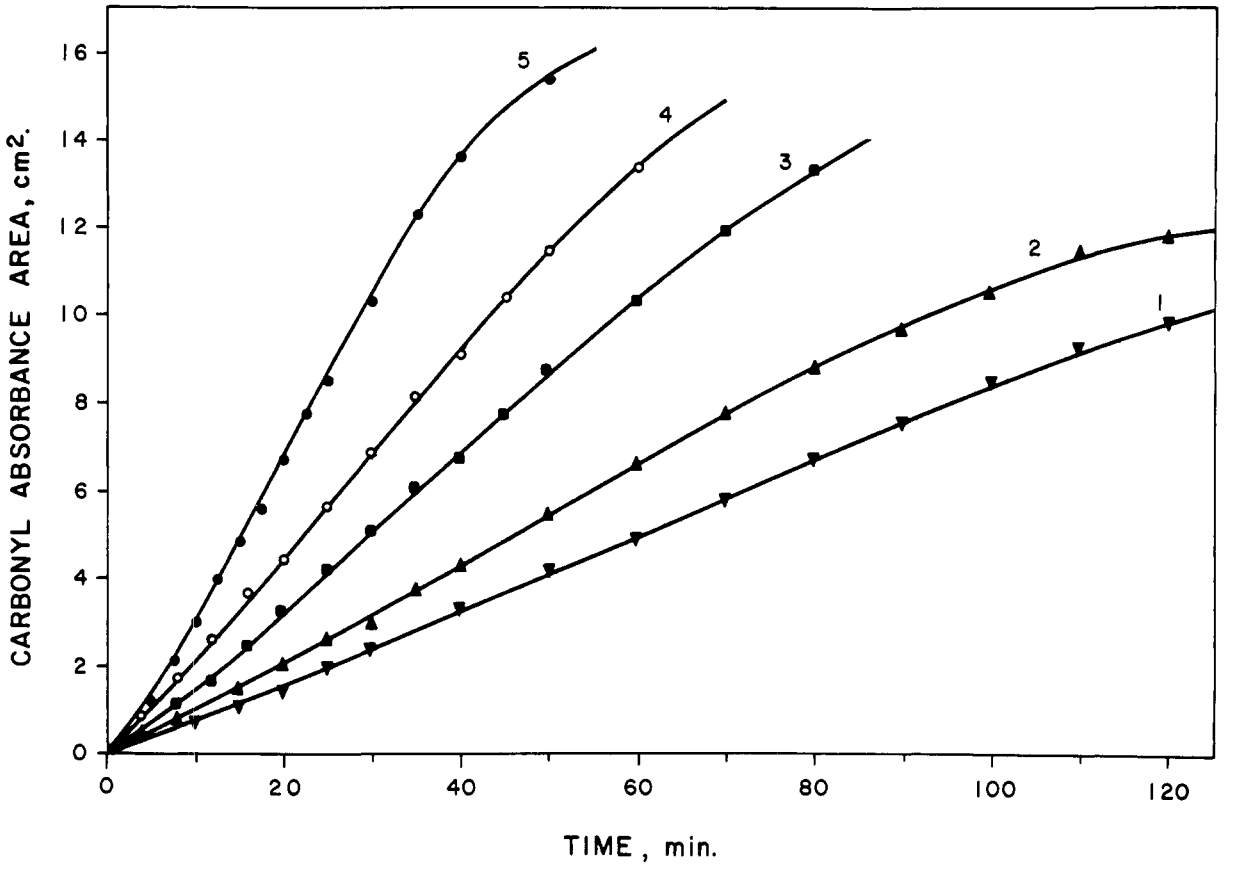


Figure 1. Carbonyl absorbance area *vs.* reaction time at 120° and [Co(III)] = $3 \times 10^{-7}$ mol/7.5 mg of APP, for various ratios of oxygen:nitrogen: 1, 5:95; 2, 10:90; 3, 25:75; 4, 50:50; 5, 100:0.

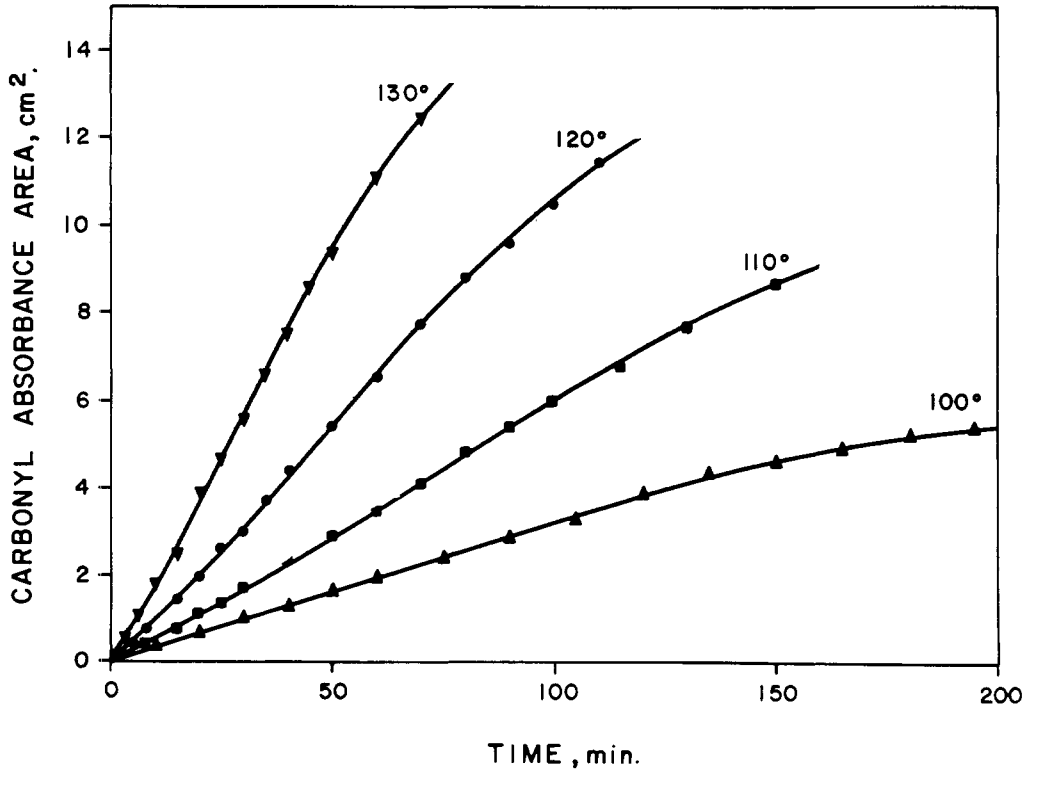


Figure 2. Carbonyl absorbance area *vs.* reaction time at oxygen:nitrogen of 10:90 for various temperatures, [Co(III)] = $3 \times 10^{-7}$ mol/7.5 mg of APP.

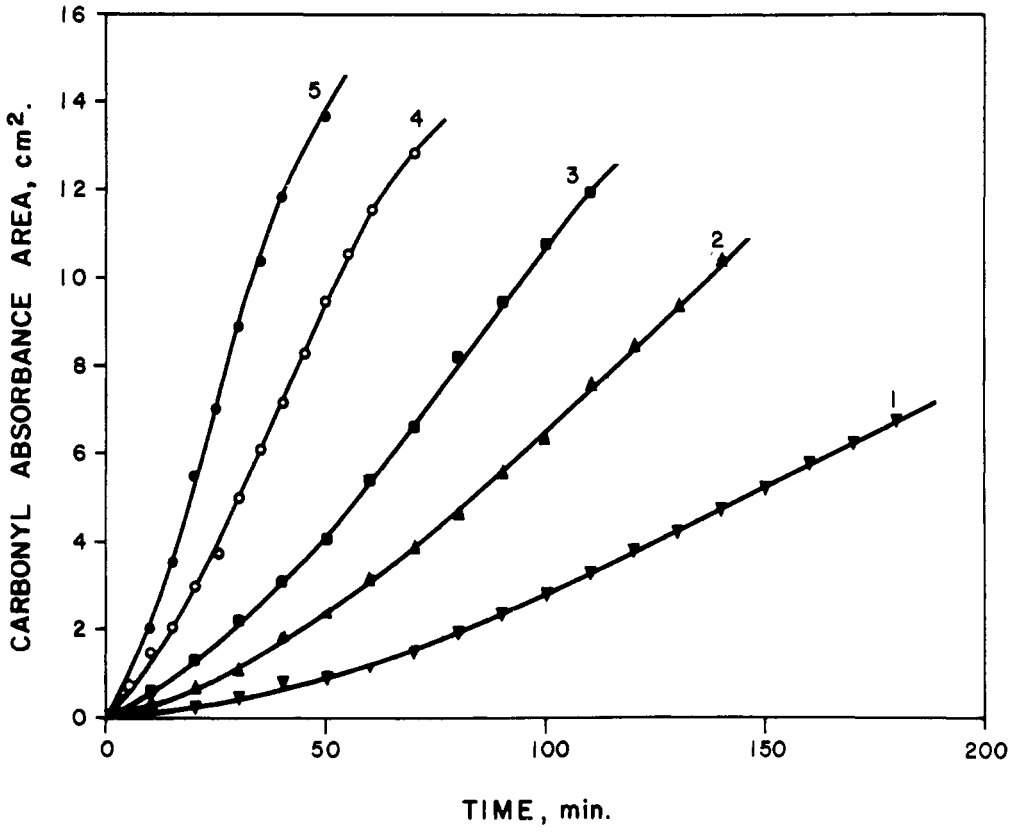


Figure 3. Carbonyl absorbance area *vs.* reaction time at 110° in pure oxygen, for various concentrations of Co(III) acetylacetonate (per 7.5 mg of APP): 1, $0.3 \times 10^{-7}$ mol; 2, $0.9 \times 10^{-7}$ mol; 3, $1.5 \times 10^{-7}$ mol; 4, $3 \times 10^{-7}$ mol; 5, $9 \times 10^{-7}$ mol.

tained during the cobalt(III) acetylacetonate catalyzed autoxidation of APP in the bulk phase.

$$\text{initiation rate} \equiv \varphi = k_i[\text{RH}][\text{O}_2][\text{Co(III)}] \quad (1)$$

$$\text{R}\cdot + \text{O}_2 \xrightarrow{k_2} \text{RO}_2\cdot \quad (2)$$

$$\text{RO}_2\cdot + \text{RH} \xrightarrow{k_3} \text{RO}_2\text{R} + \text{H}\cdot \text{ (one R can be H)} \quad (3)$$

$$\text{RO}_2\cdot + \text{RH} \xrightarrow{k_4} \text{inactive products} \quad (4)$$

$$\text{RO}_2\cdot + \text{Cat.} \xrightarrow{k_4'} \text{inactive products} \quad (4')$$

$$\text{RO}_2\text{R(RO}_2\text{H)} + \text{Co(III)} \xrightarrow{k_5} \text{RO}_2\cdot + \text{Co(II)} + \text{R}^+ \quad (5)$$

$$\text{RO}_2\text{R(RO}_2\text{H)} + \text{Co(II)} \xrightarrow{k_5'} \text{RO}\cdot + \text{Co(III)} + \text{RO}^- \quad (5')$$

$$\text{RO}_2\text{R(RO}_2\text{H)} + \text{Cat.} \xrightarrow{k_6} \text{inactive nonvolatile products (>C=O, -CHO, etc.)} \quad (6)$$

$$\text{RO}_2\text{R(RO}_2\text{H)} \xrightarrow{k_{6a}} \text{inactive nonvolatile products (>C=O, -CHO, etc.)} \quad (6a)$$

$$\text{RO}\cdot \xrightarrow{k_7} \text{R}\cdot' + \text{volatile products} \quad (7)$$

$$\text{R}\cdot' + \text{RH} \xrightarrow{k_8} \text{R'H} + \text{R}\cdot \quad (8)$$

$$\text{R}\cdot' + \text{O}_2 \xrightarrow{k_9} \text{R'O}_2\cdot$$

$$2\text{R'O}_2\cdot \xrightarrow[\text{fast}]{\text{very}} \text{products} \quad (9)$$

$$\text{R}\cdot' + \text{R'O}_2\cdot \xrightarrow[\text{fast}]{\text{very}} \text{R'O}_2\text{R'}$$

In eq 1, the initiation step is assumed to provide R· radicals. (The assumption of $RO_2$· radicals will not greatly affect the kinetic expressions derived subsequently.) Bawn and Chaudhri[6] postulated a similar initiation step but employed a Mn(III) salt. Further, Betts and Uri[13] postulated an initiation step to account for the autoxidation of several hydrocarbons which involved Co(II) complexes. Steps 2–4, 6a, 7, and 8 have been previously reported for the uncatalyzed autoxidation of various polyolefins.[2a] In step 3, we have arbitrarily maintained that $RO_2R$ can form as well as $RO_2H$, although the latter is energetically favored, since in either case the derived kinetic expressions will not change much. Steps 4 and 4′ have been included to account for the deactivation of $RO_2$· radicals by inherent impurities in the substrate, RH, and by the catalyst, Cat., respectively. No differentiation is made as to the oxidation state of the catalyst molecule which undergoes this deactivation reaction. Other workers have also postulated a deactivation step such as (4′) to account for the metal salt catalyzed autoxidation of tetralin. Thus, Kamiya and Ingold[14] studied the autoxidation of tetralin in chlorobenzene at 65° as a function of cobalt(II) decanoate concentration. At relatively high metal catalyst concentrations, it was found that after a critical catalyst concentration, the maximum autoxidation rate dropped catastrophically. This was attributed, in part, to a chain-termination process similar to step 4′. Steps 5 and 5′ have been frequently utilized for the metal-catalyzed autoxidation

(13) A. T. Betts and N. Uri, *Makromol. Chem.*, **95**, 22 (1966).
(14) Y. Kamiya and K. U. Ingold, *Can. J. Chem.*, **42**, 2424 (1964).

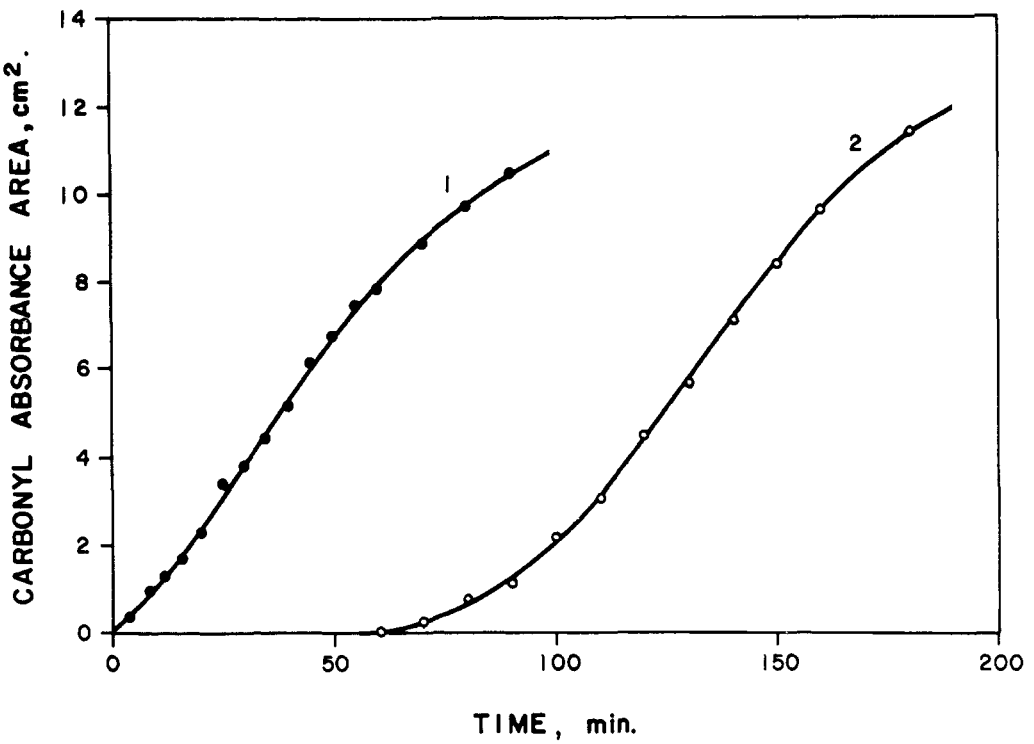


Figure 4. Carbonyl absorbance area *vs.* reaction time at 110° and oxygen:nitrogen of 50:50: 1, [Co(III)] = 3 × $10^{-7}$mol/7.5 mg of APP; 2, [Co(II)] = 3 × $10^{-7}$ mol/7.5 mg of APP.

of various hydrocarbons.[2a] Kamiya[15] has postulated a reaction similar to step 6 during the metal-catalyzed autoxidation of tetralin. Further, on the basis of previous work,[16] the authors have found a good correlation between oxidation potential of various metals with maximum rate of nonvolatile carbonyl formation during the autoxidation of APP in the bulk phase. Since metals react with $RO_2H$ readily, it is reasonable to assume that a reaction such as step 6 is occurring leading to the formation of nonvolatile carbonyl-containing compounds. In eq 7, it is postulated that the tertiary alkoxy radical of APP decomposes into smaller radical fragments, R·′, and volatile products. Recently, Carlsson and Wiles[17] subjected powdered, unstabilized polypropylene to air for 1–5 min at 225° and indicated that, based upon infrared absorption spectra, two principal ketone products were formed (presumably from the tertiary alkoxy radical of polypropylene). One of these products was apparently formed by loss of a methyl radical while the other ketone product could form by chain cleavage. Both ketones were present in about equal amounts. The formation of a methyl radical, as opposed to an alkyl radical, would not be anticipated based upon free-radical chemistry of simple hydrocarbons in solution. In view of this and because of the much lower reaction temperatures used in our work (100–130°), we have postulated that the RO· radical in step 7 undergoes chain scission predominantly to afford a low molecular weight radical (of relatively high mobility in the bulk polymer) and a relatively low molecular weight product which can volatilize under our experimental conditions. With respect to eq 9, it may be mentioned that we previously[2] indicated that R·′ + $O_2$ → less active products. In this paper, we are elucidating this step by showing the formation of $R'O_2$· radicals which terminate rapidly to yield products (the $R'O_2$· radicals are presumably of much greater mobility than polymeric $RO_2$· radicals). We are also including a cross-termination step since the R·′ is also a mobile species. However, the bimolecular reaction involing the $R'O_2$· would be favored because of formation of peroxide radicals in an oxidizing medium. The formation of $R'O_2$· radicals is considered to be rate controlling. The question of unimolecular *vs.* bimolecular termination in the polymer matrix is still moot. However, bimolecular terminations are well known in free-radical chemistry and are, therefore, favored in step 9. Because of the rapid consumption of $R'O_2$· radicals in the termination step 9 the reaction $R'O_2$· + RH would likely be deterred and is therefore not included in the general scheme.

It was experimentally observed (Figure 4) that when the Co(II) salt was used as catalyst, there was a relatively long induction period (*ca.* 50 min) followed by a rapid increase in rate of carbonyl formation to a maximum value ($\rho_m$) of 13.5 $cm^2$/min. Under identical conditions, the Co(III) salt showed virtually no induction period ($\rho_m$ = 15 $cm^2$/min). Thus, the latter valence form is the more effective catalyst. Since the catalyst is added in the Co(III) form and any Co(II) produced during the oxidation would be converted into the higher valence state, we may write

$$k_5[\text{Co(III)}] \equiv k_5[\text{Cat.}] = k_5'[\text{Co(II)}] \qquad (10)$$

In obtaining eq 10, it has been assumed that steady-state

(15) Y. Kamiya, *Bull. Chem. Soc. Jap.*, **38**, 2156 (1965).
(16) L. Reich, B. R. Jadrnicek, and S. S. Stivala, *J. Polym. Sci.*, in press.
(17) D. J. Carlsson and D. M. Wiles, *Macromolecules*, **2**, 587 (1969).

conditions apply and that steps 4′ and 6 are of relatively minor importance in comparison with steps 5 and 5′ ($k_5 \gg k_6$). Further, eq 10 would be more valid at relatively low conversions. Also, from the scheme, assuming steady-state conditions for [R·], [R·′], and [$RO_2$·]

$$[RO_2\cdot] = \frac{\varphi}{(k_3 + k_4)[RH] + k_4'[Cat.]} + \frac{k_5[Cat.][RO_2R](2k_8[RH] + k_9[O_2])}{(k_8[RH] + k_9[O_2])\{(k_3 + k_4)[RH] + k_4'[Cat.]\}} \quad (11)$$

The rate of hydroperoxide formation may be written as

$$d[RO_2R]/dt = k_3[RO_2\cdot][RH] - (2k_5 + k_6)[Cat.][RO_2R] - k_{6a}[RO_2R] \quad (12)$$

Upon substituting eq 11 into 12 and integrating, there is obtained

$$[RO_2R] = (B/A)(1 - e^{-At}) \quad (13)$$

where

$$A \equiv (2k_5 + k_6)[Cat.] + k_{6a} - \frac{k_3k_5[Cat.][RH]}{(k_3 + k_4)[RH] + k_4'[Cat.]}\left(\frac{2k_8[RH] + k_9[O_2]}{k_8[RH] + k_9[O_2]}\right)$$

$$B \equiv k_3[RH]\varphi/(k_3 + k_4)[RH] + k_4'[Cat.]$$

From eq 13, the maximum concentration of hydroperoxide, $[RO_2R]_m$, at time $t_m$ may be written as

$$[RO_2R]_m = [B/(k_{6a} + A_0[Cat.])](1 - e^{-At_m}) \quad (14)$$

where

$$A_0 \equiv (A - k_{6a})/[Cat.]$$

Now, let the maximum rate of carbonyl formation, $(d[>C{=}O]/dt)_m$, be denoted by $\rho_{m,tot}$, where

$$\rho_{m,tot} \equiv \rho_{m,M} + \rho_{m,0} \quad (15)$$

and

$$\rho_{m,M} \equiv k_6[Cat.][RO_2R]_m$$

$$\rho_{m,0} \equiv k_{6a}[RO_2R]_m$$

Combining eq 14 and 15 and assuming $A_0/k_6 \gg 1$, we obtain

$$(\rho_{m,tot} - \rho_{m,0}) = \rho_{m,net} = \frac{k_6k_3[RH]\varphi(1 - e^{-At_m})/(k_3 + k_4)[RH] + k_4'[Cat.]}{2k_5 + k_6 - \left(\frac{k_3k_5[RH]}{(k_3 + k_4)[RH] + k_4'[Cat.]}\right)\left(\frac{2k_8[RH] + k_9[O_2]}{k_8[RH] + k_9[O_2]}\right)} \quad (16)$$

In the derivation of eq 16, it was also assumed that the value of $[RO_2R]_m$ for the uncatalyzed oxidation is of the same order of magnitude as that for the metal-catalyzed autoxidation under similar experimental conditions. This was experimentally verified. Thus, the following values of $[RO_2R]_m$ (as peroxidic oxygen) were obtained: at 120° and an $O_2$:$N_2$ ratio of 100:0, values of $[RO_2R]_m$ = 0.79 wt % for the uncatalyzed oxidation and, for the catalyzed oxidation, $[RO_2R]_m$ = 0.75 wt %; at 130° and an $O_2$:$N_2$ ratio of 100:0, values of $[RO_2R]_m$ = 0.91 wt % for the uncatalyzed reaction and, for the catalyzed oxidation, $[RO_2R]_m$ = 0.85 wt %. In both cases of catalyzed oxidation, [Co(III)] = $3 \times 10^{-7}$ mol/7.5 mg of APP. Further, in the subsequent use of eq 16, it was assumed that $At_m \approx$ constant under the various experimental conditions employed. This was justified as follows. If we assume that $A \gg k_{6a}$ (*cf.* eq 14) then at constant [Cat.], $At_m$ is directly proportional to $A_0t_m$, where $A_0 = (2k_5 + k_6)\psi \approx 2k_5\psi$ (*cf.* eq 10) and $\psi \equiv 1 - \beta(2K_3 + [O_2]/K_3 + [O_2])$ (see eq 17 for the definitions of $K_3$ and $\beta$). At any particular temperature and various $O_2$:$N_2$ ratios, it was found that $\psi t_m$ (and hence $At_m$) was approximately constant. In order to correct for temperature effects, it was assumed that $E_5$ (activation energy corresponding to step 5 and $k_5$) was 24 kcal/mol.[5] Thus, it was found that $k_5$ increased by a factor of 2.1 for every 10° increase in reaction temperature. Using this factor, values of $K_3$ and $\beta$, and 110° as a basis for comparison, it was found that an average value of $(A_0t_m)_{110°}/(A_0t_m)_T$ = 1.0 ± 0.15 was obtained over a range of temperatures ($T$) of 100–130° and for $O_2$:$N_2$ ratios of 5:95–100:0 at a value of [Cat.] = $3 \times 10^{-7}$ mol/7.5 mg of APP.

In a similar manner, it was found that $A_0$[Cat.]$t_m$ (and hence $At_m$) was constant at 110° and 100% oxygen for various values of [Cat.]. Thus, the ratio $(t_m[Cat.]_s)/(t_m[Cat.])$ was found to be about 1.0 ± 0.14 over a range of values of [Cat.] of (0.3–82.0) $\times 10^{-7}$ mol/7.5 mg of APP relative to $[Cat.]_s = 3 \times 10^{-7}$ mol/7.5 mg of APP. Various simpler expressions may be derived from eq 16 depending upon experimental conditions employed.

**Rate Dependence on Oxygen Concentration.** When [RH], [Cat.], and temperature are all constant, eq 16 reduces to

$$\rho_{m,net} = \frac{\alpha\varphi}{1 - \beta\left(\frac{2K_3 + [O_2]}{K_3 + [O_2]}\right)} \quad (17)$$

where

$$K_3 \equiv k_5[RH]/k_9$$

$$\alpha \equiv \frac{k_3[RH](1 - e^{-At_m})}{(k_3 + k_4)[RH] + k_4'[Cat.]}\left(\frac{k_6}{2k_5 + k_6}\right)$$

$$\beta \equiv \frac{k_3[RH]}{(k_3 + k_4)[RH] + k_4'[Cat.]}\left(\frac{k_5}{2k_5 + k_6}\right)$$

(a) When oxygen concentration is relatively high, *i.e.*, $(1 - \beta)[O_2] \gg (1 - 2\beta)K_3$, eq 17 becomes

$$\rho_{m,net} = \alpha_1K_3 + \alpha_1[O_2] \quad (18)$$

where $\alpha_1 \equiv \alpha k_i[RH][Cat.]/(1 - \beta)$.

(b) When oxygen concentration is relatively low, *i.e.*, $(1 - \beta)[O_2] \ll (1 - 2\beta)K_3$, eq 17 reduces to

$$\rho_{m,net} = \frac{\alpha_1(1 - \beta)}{(1 - 2\beta)}[O_2] = \alpha_2[O_2]/(1 - 2\beta) \quad (19)$$

where $\alpha_2 \equiv \alpha_1(1 - \beta)$.

**Rate Dependence on Catalyst Concentration.** When [RH], [$O_2$], and temperature are all constant, eq 16 becomes

$$\rho_{m,net} = C_1[Cat.]/k_4'[Cat.] + C_2[RH] \quad (20)$$

where

$$C_1 \equiv k_3[\mathrm{RH}]^2(1 - e^{-A t_m})\left(\frac{k_6}{2k_5 + k_6}\right)k_i[\mathrm{O_2}]$$

$$C_2 \equiv (k_3 + k_4) - k_3\left(\frac{k_5}{2k_5 + k_6}\right)\left(\frac{2K_3 + [\mathrm{O_2}]}{K_3 + [\mathrm{O_2}]}\right)$$

(a) When catalyst concentration is relatively low, *i.e.*, $k_4'[\mathrm{Cat.}] \ll C_2[\mathrm{RH}]$, eq 20 now becomes

$$\rho_{m,net} = (C_1/C_2[\mathrm{RH}])[\mathrm{Cat.}] \quad (21)$$

(b) When catalyst concentration is relatively high, *i.e.*, $k_4'[\mathrm{Cat.}] \gg C_2[\mathrm{RH}]$, eq 20 now becomes

$$\rho_{m,net} = C_1/k_4' = \text{constant} \quad (22)$$

## Results and Discussion

The rate of carbonyl formation was strongly influenced by the addition of cobalt acetylacetonate. Contrary to the uncatalyzed oxidation of APP,[3] it was generally observed in the metal-catalyzed oxidation of APP that the induction periods were of much shorter duration, when they existed, under similar experimental conditions. Thus, at an $O_2$:$N_2$ ratio of 10:90 and at 130°, an induction time of *ca.* 30 min obtained for the uncatalyzed oxidation[3] whereas an induction time of *ca.* 5 min obtained for the catalyzed oxidation ($3 \times 10^{-7}$ mole of Co(III)/7.5 mg). Maximum rates of formation of total carbonyl were determined from plots of carbonyl absorbance area *vs.* time for various catalyst and oxygen concentrations and temperatures (*cf.* Figures 1–3). From these maximum rates were subtracted values of the maximum rates reported in a previous paper for the uncatalyzed oxidation of APP, in order to obtain $\rho_{m,net}$ (see Table I of ref 3).

**Rate Dependence on Catalyst Concentration.** From eq 21, a plot of $\rho_{m,net}$ *vs.* [Cat.] should afford a linear relationship, at relatively low values of [Cat.], whose kinetic dependency with respect to [Cat.] should be first order. Figure 5 shows a plot of log $\rho_{m,net}$ *vs.* log [Co(III)]. When only the relatively low values of [Co(III)] are included in this plot, the kinetic order with respect to [Co(III)] was found to be 1.0 (*cf.* Figure 5), as anticipated, over a range of [Cat.] from (3 to 45) $\times 10^{-8}$ mol/7.5 mg of sample (0.024–0.36 wt % as Co) and at 110° and an $O_2$:$N_2$ ratio of 100:0. It may be interesting to note here that when log $\rho_{m,tot}$ was plotted against log [Co(III)], a kinetic order with respect to the latter of 0.6 was obtained. In this connection may be mentioned the work of Bawn and Chaudhri.[6] These investigators observed that when the logarithm of the observed maximum rate of oxygen uptake was plotted against log [Mn(III)], a kinetic order of 0.6 was obtained with respect to the latter. However, we have estimated that a kinetic dependency close to unity can be obtained from the data of Bawn and Chaudhri when from the maximum rate of oxygen uptake for the metal-catalyzed oxidation is subtracted the appropriate value of the maximum rate for the uncatalyzed reaction.[18]

At relatively high values of [Cat.], eq 22 should be applicable. From this expression, it can be seen that $\rho_{m,net}$ should be constant at high [Cat.]. This can be observed from Figure 5. Thus, at 110° and an $O_2$:$N_2$ ratio of 100:0, the kinetic dependency of $\rho_{m,net}$ upon [Cat.] was found to be −0.1 (*cf.* curve 1 of Figure 5) for a range of [Cat.] from (0.9 to 8.2) $\times 10^{-6}$ mol/7.5 mg of APP sample. It is noted from eq 20 and 22 that $\rho_{m,net}$ at high [Cat.] should be directly proportional to oxygen concentration. This relationship was found to apply as shown in Figure 5. Thus, when the autoxidation was carried out at an $O_2$:$N_2$ ratio of 50:50 under experimental conditions otherwise similar to those of the 100% $O_2$ oxidation, $\rho_{m,net}$ (av) was reduced by a factor of 0.50, as anticipated (*cf.* curve 2 of Figure 5). From curve 2, a kinetic dependency of −0.06 was observed with respect to [Cat.].

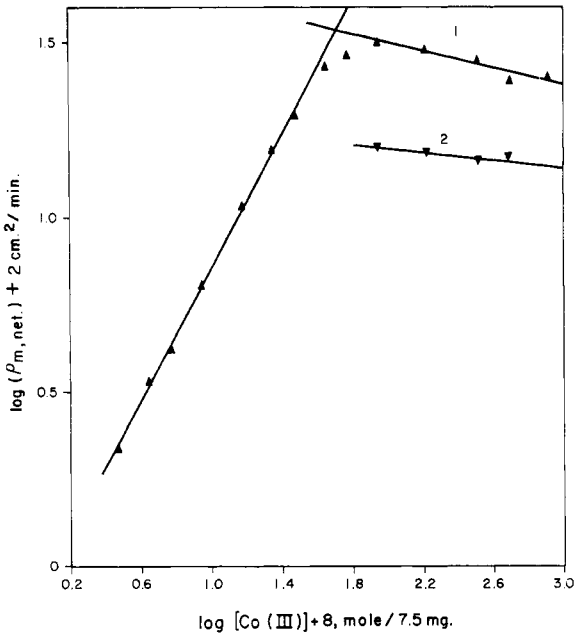


Figure 5. Relationship between the maximum rate and the concentration of Co(III) acetylacetonate at 110° and oxygen:nitrogen of 100:0 (1) and 50:50 (2).

**Rate Dependence on Oxygen Concentration.** Equation 17 may be rewritten as

$$\rho_{m,net} = \frac{\alpha_2[\mathrm{O_2}](K_3 + [\mathrm{O_2}])}{K_3(1 - 2\beta) + [\mathrm{O_2}](1 - \beta)} \quad (17a)$$

Prior to correlating $\rho_{m,net}$ as a function of oxygen concentration, it is necessary to estimate the constants $K_3$, $\alpha_2$, and $\beta$ in eq 17a. It should be possible from eq 18 to estimate $K_3$ for high values of [$O_2$] by plotting $\rho_{m,net}$ *vs.* [$O_2$], Figure 6. These values of $K_3$ should be identical with corresponding $K_3$ values previously reported for the uncatalyzed oxidation of APP[3] under similar experimental conditions. In the following are listed $K_3$ values (*cf.* Table I) for the catalyzed and uncatalyzed oxidations and various reaction temperatures, respectively: 39, 35, 110°; 42, 44, 120°; and 50, 58, 130°. Although the agreement appears to be satisfactory, we prefer to utilize $K_3$ values from the uncatalyzed oxidation since the experimental error is less for this oxidation (*cf.* Table I of ref 3). (This would be anticipated because of the much slower rates of carbonyl formation encountered in the uncatalyzed reaction.) From such values of $K_3$, values of $\alpha_2$ and $\beta$ can be estimated as

(18) C. E. H. Bawn and S. A. Chaudhri, *Polymer*, **9**, 123 (1968).

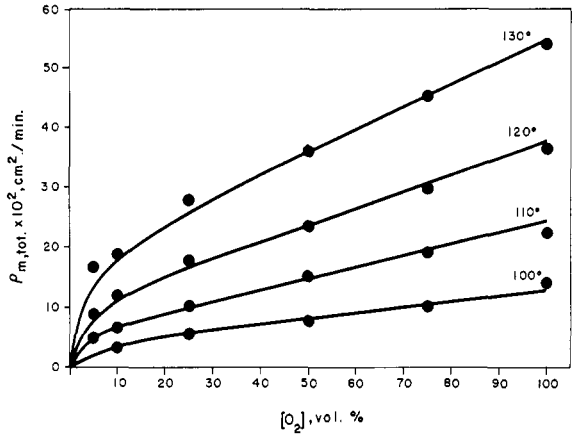


Figure 6. Effect of oxygen concentration on the maximum rate at various temperatures: [Co(III)] = $3 \times 10^{-7}$ mol/7.5 mg of APP.

follows. For the uncatalyzed oxidation of APP, it has been reported[3] that the maximum rate of carbonyl formation may be expressed as

$$\rho_{m,0} = \frac{K_1[O_2]}{1 - \dfrac{K_2}{K_3 + [O_2]}} \tag{23}$$

where the parameters $K_1$ and $K_2$ have been previously defined in eq 7a and 7b of ref 3. (Also see ref 2a.) When eq 17a is divided by eq 23, the following is obtained

$$\frac{\rho_{m,net}}{\rho_{m,0}} \equiv R = \frac{\alpha_2(K_3 - K_2 + [O_2])}{K_1\{K_3(1 - 2\beta) + [O_2](1 - \beta)\}} \tag{24}$$

From eq 24, at high values of $[O_2]$

$$R \approx \alpha_2/K_1(1 - \beta) \tag{25}$$

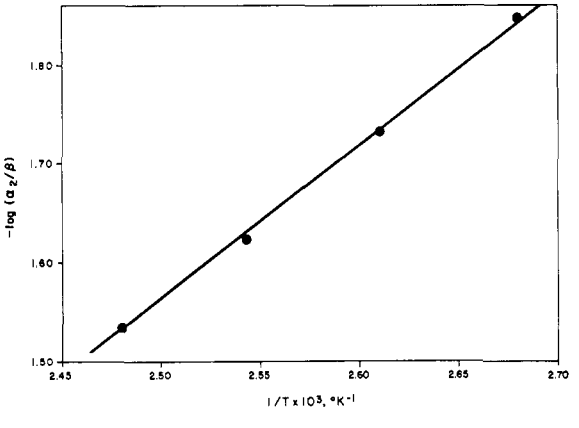


Figure 7. Plot of log $(\alpha_2/\beta)$ *vs.* reciprocal temperature, $1/T$.

TABLE I
VALUES OF $\alpha_2$ AND $\beta$ UNDER VARIOUS EXPERIMENTAL CONDITIONS

| Reaction temp, °C | $K_1 \times 10^4$,[a] cm²/min | $K_2$ | $K_3$ | $\alpha_2 \times 10^4$,[a] cm²/min | $\beta$ |
|---|---|---|---|---|---|
| 100 | 1.26 | 17.0 | 25.7 | 6.65 | 0.471 |
| 110 | 2.15 | 27.0 | 34.9 | 8.78 | 0.476 |
| 120 | 5.50 | 35.2 | 44.0 | 11.42 | 0.481 |
| 130 | 9.20 | 48.6 | 57.6 | 14.10 | 0.486 |

[a] Arbitrary units depending upon the scale utilized in obtaining carbonyl absorbance areas.

while at low values of $[O_2]$

$$R \approx \alpha_2(K_3 - K_2)/K_1K_3(1 - 2\beta) \tag{26}$$

From eq 25 and 26, it should be possible to estimate values of $\alpha_2$ and $\beta$ utilizing previously reported[3] values of $K_1$ and $K_2$ (and $K_3$); *cf.* Table I. In this manner were estimated values of $\alpha_2$ and $\beta$ which are listed in Table I for various experimental conditions. Values of $R$ at high $[O_2]$ were calculated at $[O_2] = 100\%$, whereas values at low $[O_2]$ were estimated at $[O_2] = 3\%$ by means of interpolation. From the values of $\alpha_2$ and $\beta$ in Table I and from eq 17a were calculated theoretical values of $\rho_{m,net}$ at various values of $[O_2]$ and reaction temperatures. In Figure 6 are shown calculated curves in plots of $\rho_{m,tot}$ (obtained from $\rho_{m,net}$) *vs.* $[O_2]$. The agreement between calculated and observed values appears to be satisfactory. (Values at 100° were obtained from extrapolated values of $K_1$, $K_2$, $K_3$, and $\rho_{m,0}$.)

Utilizing the definitions of $\alpha_2$ and $\beta$ (*cf.* eq 17 and 19), an Arrhenius plot of log $(\alpha_2/\beta)$ *vs.* reciprocal temperature, $1/T$, should afford an activation energy, $E$, which is equal to $E_i + E_6 - E_5$. Figure 7 shows such a plot. From this figure, $E = 7$ kcal/mol. For the uncatalyzed reaction $E = 17$ kcal/mol (this $E$ also involves the initiation step as well as steps 5 and 6 for the uncatalyzed reaction). In this connection, lower $E$ values may be anticipated for the catalyzed reaction, since $E_i$ for the catalyzed oxidation should be of lower magnitude than the corresponding value for the initiation step of the uncatalyzed oxidation, and if it is assumed that $E_6 - E_5$, which involves steps 5 and 6 for both catalyzed and uncatalyzed reactions, is of a similar order of magnitude for catalyzed as well as uncatalyzed oxidations. Finally, it may be mentioned that a value of $E = 13$ kcal/mol was obtained during the uncatalyzed autoxidation of isotactic polybutene-1.[5] In this oxidation, a relatively large amount of metallic ash was observed (*ca.* 0.17%).

**Acknowledgment.** This work was supported, in part, by a grant from the Office of Naval Research to Stevens Institute of Technology.